RSC Advances

ROYAL SOCIETY OF CHEMISTRY

www.rsc.org/advances

HSAF-induced antifungal effects in *Candida albicans* through ROS-mediated apoptosis

Yanjiao Ding,[a] Zhenyu Li,[a] Yaoyao Li,[a] Chunhua Lu,[a] Haoxin Wang,[b] Yuemao Shen,[a,b,*] and Liangcheng Du[c,*]

[a]*Key Laboratory of Chemical Biology (Ministry of Education), School of Pharmaceutical Sciences, Shandong University, No. 44 West Wenhua Road, Jinan, Shandong 250012, P. R. China*

[b]*State Key laboratory of Microbial Technology, Shandong University, No. 27 South Shanda Road, Jinan, Shandong 250100, P. R. China*

[c]*Department of Chemistry, University of Nebraska-Lincoln, Lincoln, NE 68588, USA*

Address correspondence to Yuemao Shen, yshen_lab@163.com; Liangcheng Du, zuorumeng@126.com

Key Words: HSAF, *Candida albican*s, reactive oxygen species, apoptosis

Abstract

Heat-stable antifungal factor (HSAF) belongs to polycyclic tetramate macrolactams (PTMs), which inhibits many fungal pathogens and is effective in inhibiting the *Candida albican*s (*C. albicans*). In this study, we found that HSAF induced the apoptosis of *Candida albican*s SC5314 through inducing the production of reactive oxygen species (ROS). Nevertheless, we validated the efficacy of HSAF against candidiasis caused by *C. albicans* in murine model in vivo, and HSAF

significantly improved survival and reduced fungal burden compared to vehicles. Molecular dynamics (MD) simulation was also investigated, revealing the theoretical binding mode of HSAF to the β-tubulin of *C. albicans*. This study first found that the PTMs-induced fungal apoptosis through ROS accumulation in *C. albicans* and its potential as a novel agent for fungicides.

Introduction

In recent decades, the incidence and frequency of invasive fungal infections were widespread and there was a sharpen increase in mortality due to mycoses, especially in the population of immuncompromised patients. Fungal infections are a major source of global morbidity and mortality, especially for the species of *Candida* and *Aspergillus*.[1] Therefore, how to treat the *C. albicans* infection has attracted the interests of the worldwide researchers. At present, the most common antifungal drugs are the azoles such as imidazoles, triazoles, voriconazole and posaconazole, which disrupt the cell membrane by inhibiting the biosynthesis of ergosterol.[2] The polyenes such as nystatin and amphotericin B bind ergosterol and destroy the fungal cell membrane. Echinocandis such as caspofungin, micafungin and anidulafungin inhibit the synthesis of fungal wall by blockage of the glucan synthase.[3] However, Candida species has been reported to show azole resistances through upregulation of efflux, mutation and overexpression to confront the variety of stress conditions.[4, 5] New anti-candida drugs with distinct chemical structures and mechanism of action are urgently required.

Heat-stable antifungal factor (HSAF) was isolated from *Lyaobacter enzymogenes* C3, a biocontrol strain for many fungal plant diseases[6] and belongs to polycyclic tetramate macrolactam (PTM), which is a tetramic acid (2,4-pyrrolidinedione)-containing macrolactam.[7] PTMs as a new emerging class of natural products have shown significant bioactivities, including antifungal, antibiotic, and antitumor properties.[8] Previously, Li and coworkers showed that HSAF induced

aberrant deposition of thick cell wall patches to inhibit the growth of *Aspergillus nidulans*, and proposed that the antifungal activity of HSAF was mediated by disrupting the biosynthesis of ceramide.[9] Though great efforts have been made to investigate the mode of action of HSAF, the cellular biological mechanisms and the target of HSAF are still unknown. Ceramides have been reported to have effects on mitochondria including enhanced generation of reactive oxygen species (ROS).[10] Recent studies have reported that major classes of antibiotics contribute to induce apoptosis via the production of ROS.[11] Therefore, to determine whether or not HSAF induced apoptosis in *C. albicans* through ROS accumulation, we investigated various apoptotic features after treatment with HSAF. In this study, we reported the antifungal activity of HSAF against filamentous pathogenic fungi, yeast and filamentous forms of *C. albicans* in vitro. Nevertheless, we validated the efficacy of HSAF against candidiasis caused by *C. albicans* in mice model in vivo. We investigated the antifungal mechanism of HSAF using RNA-seq technology, morphological, and molecular assays to confirm its mode of action and found that HSAF exhibited potent anti-Candida activity, arresting cells at G2/M phase and triggering apoptosis via an ROS dependent pathway.

Experimental section

Fungal strains and growth conditions

The filamentous pathogenic fungi were maintained on potato dextrose agar (PDA) medium including 20% potato, 2% dextrose and 2% agar at 25 ℃ for 5 d. *C. albicans* (ATCC 5314) were used for all experiments described and were cultured in YPD

medium containing 1% yeast extract, 2% peptone, and 2% dextrose with 250 rpm at 28 °C, overnight. *C. albicans* cultures were grown to an optical density 600 of 0.1 to 1.0 and diluted, coated plates, counted to determine the relationship between OD_{600} and Log CFU/mL. *C. albicans* cultures were diluted into the YPD and grown to an optical density 600 of 0.2, at which point the HSAF were added. The Minimum Inhibitory Concentrations (MICs) were determined using the Clinical and Laboratory Standards Institute (CLSI) method.[12]

Total RNA extraction and high throughput sequencing

Total RNA (~10 μg) was extracted using fungal RNA kit (OMEGA BIO-TBK) according to the manufacturer's instructions. The RNA quality and quantity were assessed using a NanoDrop-Spectrophotometer ND-1000 (NanoDrop Technologies, Wilmington, DE, USA). A260/280 ratio (approx. 1.8-2.0) for RNA samples calculated by Nanodrop was also considered to check quality of the RNA preparation. RNA-seq libraries were prepared and sequenced by Macrogen, Inc. (South Korea) with the Illumina HiSeq 2000 technology. To study the global effect of HSAF, cells were exposed to HSAF concentration (10 μg/mL) over 20 h. At 10 and 20 h, whole-cell RNA was sequenced for both control- and HSAF-exposed cells with ~30 million 50-bp paired-end reads generated per sample.

Assay for germ tube formation

A colony of *C. albicans* SC5314 was used to inoculate 2 mL of YPD medium. The cells were incubated for at least 48 h at 25 °C without shaking and then centrifuged for 5 min at 2000 *g* to pellet the cells. The pellet was then resuspended

with RPMI 1640. The cells of *C. albicans* were diluted to OD_{600} = 0.2 and dispensed into a 96-well flat-bottom polystyrene plate. Samples were treated with 1.5, 3 and 6 μg/mL HSAF with dimethyl sulfoxide at a final concentration of 1%. The plate was placed in a 37 °C incubator for 4 h without shaking.[13] Germ tube attached to the wells were stained with 100 μL of 0.02% crystal violet dissolved in phosphate-buffered saline (PBS) for 15 min and then analyzed by ZEISS fluorescence microscope (ZEISS, Axio Observer A1, Germany) using a 40 × objective.

Measurement of ROS production in *C. albicans*

C. albicans cells were treated with HSAF using 2', 7'-dichlorfluorescin diacetate (DCFH-DA) to measure the endogenous ROS. Logarithmically growing *C. albicans* cells were treated with 3, 6 and 12 μg/mL HSAF or DMSO in YPD for 1, 2 and 3 h at 28 °C, after that cells were washed with PBS (pH 7.4) three times and DCFH-DA was added which final concentration with 10 μM in PBS. After 30 min incubation at 28 °C, samples were quantitatively analyzed with a flow cytometer (Becton Dickinson, San Jose, CA, USA).

Measurement of mitochondrial membrane potential ($\Delta\Psi m$)

$DiOC_6(3)$ was used as the marker to measure the effect of HSAF on the mitochondrial membrane potential of *C. albicans*. Cells were harvested and incubated with 3, 6 and 12 μg/mL HSAF or DMSO for 3 h at 28 °C. After that, cells were washed with PBS (pH 7.4) three times and incubated with 100 nM $DiOC_6(3)$ for 30 min. Samples were analyzed by flow cytometer (Becton Dickinson, San Jose, CA, USA) as previously described.[14]

Cell cycle analysis by flow cytometry

The DNA content was quantified by the flow cytometry of the cells stained with the DNA-specific fluorescent dye propidium iodide (PI). The exponential phased cells of *C. albicans* were grown in YPD medium and then harvested and treated with 3, 6 and 12 μg/mL HSAF, meanwhile adding 1 mM and 5 mM ascorbic acid (AA) for 30 min prior to the addition of 12 μg/mL HSAF. After incubation for 3 h, the cells were washed with PBS three times and fixed with 70% ethanol overnight at -20 ℃. The cells were treated with 100 μg/mL RNase A for 2 h at 37 °C and added 50 mg/mL PI for 1 h at 4 °C in the dark. The samples were analyzed in a FACScan flow cytometer (Becton Dickinson, San Jose, CA, USA). The values represented the average of the measurements conducted in triplicate for three independent assays.

Analysis of early and late apoptotic markers

C. albicans cells were digested with lywallzyme and lysis enzyme for 2 h at 28 °C. Protoplasts were incubated with 3, 6, 12 and 24 μg/mL HSAF or DMSO for 4, 8 h at 28 °C, meanwhile adding 1 mM and 5 mM ascorbic acid (AA) for 30 min prior to the addition of 24 μg/mL HSAF. Subsequently, the cells were washed with PBS (pH 7.4) three times and incubated with 5 μL FITC-Annexin Ⅴ and 5 μL PI for 20 min in the dark. Meanwhile, 10 μg/mL amphotericin B (AMB) was as positive control. After that, cells were washed with PBS (pH 7.4) three times and observed by fluorescence microscope (OLYMPUS, IX71, Japan) using a 63 × objective.

DNA fragmentation was analyzed by the terminal deoxynucleotidyl transferase dUTP nick-end labeling method.[15] Samples were treated with 3, 6, 12 and 24 μg/mL

HSAF for 4 or 8 h, meanwhile adding 1 mM and 5 mM ascorbic acid (AA) for 30 min prior to the addition of 24 μg/mL HSAF and then washed with PBS three times, permeabilized in a permeabilization buffer (0.1% sodium citrate and 0.1% Triton X-100) on ice for 10 min and washed again with PBS three times. DNA ends were labeled with an in situ cell death detection kit at 37 °C for 1 h. Nuclear condensation was analyzed by DAPI staining[16] and then analyzed by fluorescence microscope (OLYMPUS, IX71, Japan) using a 63 × objective.

Polymerization assay

The ability of tubulin to polymerize into microtubules can be followed by observing an increase in optical density of a tubulin solution at OD_{340}. Tubulin protein from porcine brain was reconstituted to 5 mg/ml with cold tubulin buffer (80 mM PIPES, pH 6.9, 2 mM $MgCl_2$, 0.5 mM EGTA). The tubulin solution (at 4°C), which was plus 5% glycerol and 1 mM GTP adding 10 μM HSAF or 10 μM vincristine (vin), was transferred into a microtiter plate, which had been pre-warmed to 37°C. Tubulin polymerization was measured by taking readings every 30 s for 30 min. Absorbance at 340 mm was monitored in the spectrophotometer.

Molecular modeling studies

All the molecular modeling were performed on a Dell Precision T5500 workstation. The molecular docking was conducted using SYBYL-X 1.1 (Tripos, St. Louis, MO, USA). The wild type and mutant strains of *C. albicans* β-tubulin proteins were built by SWISS-MODEL, a fully automated protein structure homology-modelling server[17-20]. The compound HSAF was optimized for

1000-generations until the maximum derivative of energy became 0.05 kcal/(mol*Å), using the Tripos force field. Charges were computed and added according to Gasteigere Hückel parameters. The optimized HSAF was docked into the binding site of *C. albicans* β-tubulin proteins by means of surflex-dock, and the default parameters were used if it was not mentioned. Then a molecular dynamic (MD) study was performed to revise the docking result.

The Amber 12 and AmberTools 13 programs[21] were used for MD simulations of the selected docked pose. Compound HSAF was first prepared by ACPYPE[22], a tool based on ANTECHAMBER for generating automatic topologies and parameters in different formats for different molecular mechanics programs, including calculation of partial charges. Then, the forcefield "leaprc.gaff" (generalized amber forcefield) was used to prepare the ligand, while "leaprc.ff12SB" was used for the receptor. The system was placed in a rectangular box (with a 10.0 Å boundry) of TIP3P water using the "SolvateOct" command with the minimum distance between any solute atoms. Equilibration of the solvated complex was done by carrying out a short minimization (1000 steps of each steepest descent and conjugate gradient method), 500 ps of heating, and 200 ps of density equilibration with weak restraints using the GPU (NVIDIA® Tesla K20c) accelerated PMEMD (Particle Mesh Ewald Molecular Dynamics) module. At last, 20 ns of MD simulations were carried out.

In vivo assay for antifungal activity

To evaluate the effect of HSAF on *C. albicans* in vivo, a total of fifty male BALB/c mice (6-8 weeks old) were obtained from the Experimental Animal Center of

Shandong University (Jinan, Shandong, China). Animals were maintained in accordance with the criteria of the Guide for the Care and Use of Laboratory Animals and approved by the Animal Care and Use Committee of Shandong University. All efforts were made to minimize the number of animals used and their suffering.

The animals were housed in cages of ten mice each. *C. albicans* was grown at 37 °C in YPD medium containing penicillin and streptomycin. Cells were centrifuged, washed in PBS. Disseminated infection was produced by lateral tail vein injection of 100 μL inoculum containing 1×10^6 cells of *C. albicans* 3 h prior to the start of antifungal therapy. HSAF was intraperitoneal injection once daily at doses of 5 mg/kg of body weight. Fluconazole (FLU) and AMB were injected in the same way as the positive control or the same volume of solvent as negative control. After 3 d of therapy, mice were euthanized, kidneys were immediately removed and weighed and homogenized in sterile PBS (containing penicillin and streptomycin) and were serially diluted 1:10. Aliquots were plated onto YPD, and following 24 h of incubation at 37 °C, fungal burden (CFU/g) was determined. The other halves of the kidneys were fixed in 10% neutral formalin solution, embedded in paraffin, and stained with Periodic Acid-Schiff stain and hematoxylin-eosin stains. In the survival arm, mice were monitored off therapy until 30 d.

Results

Antifungal activities of HSAF in vitro

HSAF (Fig. 1A) exhibited antifungal activity against broad range of plant pathogenic fungi, including *P. grisea, F. verticillioide, R. solani,* and *S. sclerotiorum*

(Fig. 1B). The MIC value of HSAF against *C. albicans* was 24 μg/mL. *C. albicans* is a dimorphicfungus, which changes from yeast to hyphal form. The yeast-to-hyphal transition starts with the formation of a germ tube, which is suggested as a potential virulence factor in their pathogenesis.[23] HSAF displayed evident inhibitory effect on the germ tube formation of *C. albicans* at the concentration of 6 μg/mL in comparison to vehicle (Fig. 1C). These results indicated that HSAF not only inhibited yeast cell growth, but also inhibit the germ tube formation of *C. albicans*.

Gene annotation and functional classification

RNA sequencing was used to determine differential gene expression in response to treatment with a low dose of HSAF. The RNA-seq analysis revealed many genes are up-regulated or down-regulated in response to HSAF (Fig. 2A). The international standardized gene functional classification system Gene Ontology (GO) provided three ontologies including biological processes, cellular components and molecular functions (Fig. 2B), which were useful for gene annotation and analysis.[24] Two-group comparison showed differential expression of a number of transcripts. Gene ontology analysis revealed significant variation in many differentially expressed transcripts across comparisons. In comparison to vehicle, maximum number of transcripts were related to cellular component (n = 1107), the number of transcripts involved in biological processes was also high (n = 1069). The heat maps showed the metabolic bases of the interaction between the cells treated with DMSO and HSAF. Among the differentially expressed genes identified, a suite of genes involved in carbohydrate metabolism and cell cycle were found to be up-regulated under HSAF, confirming the

significance of this compound in the ROS pathway (Fig. 2C).

RNA-seq technology provided a useful tool for transcriptome analysis and it offered broad and deep insights into gene regulatory networks and biological pathways.[24] Based on transcriptional sequencing and analysis, we first identified differentially expressed genes (DEGs) between the untreated and treated cells with HSAF. Moreover, we identified important regulatory genes involved in the ROS pathway. These results will be helpful for elucidating the molecular mechanisms of HSAF effecting on fungi.

HSAF induced total intracellular ROS levels increasing and triggered collapse of mitochondrial membrane potential ($\Delta\Psi m$)

In order to determine if the mechanism of killing by HSAF was ROS mediated, we examined ROS levels of *C. albicans* cells treated with or without HSAF by fluorimetric assay. Generation of ROS was monitored by incubation of HSAF at 3, 6 and 12 μg/mL with the *Candida* cells for 1, 2, and 3 h, respectively. ROS levels were slightly elevated in *Candida* cells after exposure to HSAF at low concentrations for 2 h. Moreover, high concentration of HSAF treatment caused a marked ROS increase in Candida cells after 2 h (Fig. 3A). These findings indicated that HSAF could induce the ROS accumulation in *C. albicans* cells in a time- and dose-dependent manner.

Previous study suggested that mitochondrial ROS triggered cell apoptosis may occur *via* formation of the mitochondrial permeability transition pore complex, a crucial step in mitochondrial demolition.[25] $DiOC_6(3)$ is a mitochondrial dye that aggregates into healthy mitochondria and fluoresces green and it is specifically used

to determine the decreases in the membrane potential of mitochondria stimuli.[26] Cells of *C. albicans* were treated with 3 μg/mL HSAF resulted in a decrease in the $\Delta\Psi m$ about 45.03 %, while the concentration of HSAF reached 12 μg/mL, HSAF could induce a significant decrease in the $\Delta\Psi m$ about 11.92 % compared to the vehicle (Fig. 3B). The result showed that HSAF effect was related to the dissipation of $\Delta\Psi m$.

To determine whether the elevated ROS in *Candida* cells contributes to HSAF-induced cell death, the anti-Candida activity of HSAF without and with the ROS scavengers, ascorbic acid (AA), acetyl cysteine (NAC), glutathione (GSH) and thiourea (TU) were examined. We found that exposing exponentially growing *C. albicans* to 0.5 mM AA or 5 mM TU, the MIC of HSAF increased to 100 μg/mL (Fig. 3C) and diminished the toxicity of HSAF, reducing killing by about 30-fold at 3 h (Fig. 3C).

HSAF induced G2 cell cycle arrest and apoptosis in *C. albicans* through inducing the production of reactive oxygen species

To study the effect of HSAF on cell cycle progression, flow cytometry analysis was performed. We observed that HSAF treatment led to more cells accumulating in G2/M phase compared with vehicle cells. The ratio of cells in G2/M phase following the treatment of 3, 6 and 12 μg/mL HSAF increased to 19.02%, 20.26% and 32.69%, compared to 12.56% in vehicle group after 3 h culture in a concentration-dependent manner (Fig. 4A). The G2-M phase delay induced by HSAF could be recovered by the supplementation of AA. The results indicated that HSAF treatment induced a significant arrest in the G2/M phases of the cell cycle through inducing the production

of ROS.

Upstream cell-cycle regulators are also involved in effector-triggered programmed cell death (PCD) in cells.[27] Thus, the further investigation for the anti-Candida mechanism of HSAF was necessary through examining PCD in *C. albicans*. Apoptosis, a physiological mode of programmed cell death, is induced by diversified cellular stimuli and through many signaling pathways.[28] In the presence of Ca^{2+}, Annexin V-FITC stain, which binds to phosphatidylserine,[29] can examine the early stage apoptosis. In the course of early apoptosis, phosphatidylserine can translocate from inner to the outer of membrane.[30] The protoplasts of *C. albicans*, which treated with 12 and 24 μg/mL HSAF after 4 h, displayed an annexin V(+)/PI(-) phenotype as an early marker of apoptosis, whereas this phenomenon was rarely observed in 3 and 6 μg/mL HSAF-treated cells for 4 h. Exposure to 3 and 6 μg/mL HSAF for 8 h caused early apoptosis in *C. albicans* (Fig. 4B). This indicated that HSAF induced early apoptosis in *C. albicans* in a time- and dose-dependent manner.

A TUNEL assay was performed to investigate nuclear morphological features of the late stage of apoptosis in *C. albicans*.[31] The cells of *C. albicans* treated with 3 μg/mL HSAF cannot induce the late apoptosis at 4 h, and the DNA fragments were observed when the cells treated with 3 μg/mL HSAF at 8 h (Fig. 4B). The cells treated with 24 μg/mL HSAF exhibited a significant amount of changed in the nuclear DNA for 4 h, consistent with the positive control, which treated with 10 μg/mL AMB, as assessed by the DNA-binding fluorescent dye DAPI (Fig. 4D). In the DMSO treated population, chromatin appeared as single round nuclei appearance. The similar results

were obtained by TUNEL assay (Fig. 4E), which is one of the most reliable ways for the identification of the late stages of apoptosis in yeast.[32] Either at early or late apoptosis stage, when added with 1 mM AA, the intensity of fluorescence changed weak, the antifungal activity of HSAF decreased, while added with 5 mM ascorbic acid, HSAF lost the antifungal activity (Fig. 4C, D, E). The results suggest that HSAF has a critical effect on apoptotic cellular changes either early or late apoptosis through inducing the accumulation of ROS. It was in a nice dose and time dependent manner.

HSAF inhibited the polymerization of β-tubulin

HSAF disrupted mitochondrial membrane potential, arrested the cell cycle at the G2/M phase, and induced apoptosis, a hallmark of microtubule destabilizing drugs.[33] Moreover, mitochondria may connect microtubule damage to the apoptotic machinery, acting as appropriate, and timing switches for the onset of apoptosis.[34] According to these observations. We tested whether HSAF directly inhibited tubulin polymerization in vitro. HSAF were assayed for inhibition of tubulin polymerization in a biochemical assay using purified tubulin isolated from porcine brain. HSAF strongly inhibited tubulin polymerization under 340 nm in vitro. A similar activity was exhibited by vinblastine (Fig. 5A).

To better elucidate the detailed interactions between HSAF and β-tubulin at the molecular level and to understand the structural basis of their binding mode, a docking study of HSAF was first performed using SYBYL-X 1.1 and then MD simulations were carried out by Amber 12. The β-tubulin-HSAF complex was equilibrated after 20 ns MD simulation, and the plot of RMSD (in ångstrom) of the

complex was shown in Fig. 5B. HSAF adopted a compact conformation to bind inside the pocket of β-tubulin (Fig. 5C). The dodecahydrocyclopenta[a]indene scaffold of HSAF fitted into the hydrophobic domain of β-tubulin, surround by residues Leu215, Lue228 and Leu273. Importantly, 7-carbonyl group and 27-carbonyl group of HSAF formed hydrogen bond interactions with residues Met276 and Ser280, respectively.

Taken together, our molecular simulation allowed us to rationalize the activity profile of the HSAF against β-tubulin, which provided valuable information for further design of novel effective β-tubulin inhibitors.

HSAF inhibited *C. albicans* in vivo

In order to relate the in vitro cytotoxicity with in vivo effects, a number of toxicity experiments were performed on a murine model of disseminated infection due to *C. albicans* with an inoculum of 1×10^6 cells/mouse. HSAF exhibited good antifungal activity in vivo. It was observed that a significant reduction in the virulence of kidney tissue of experimental mice compared to vehicle (Fig. 5). The effect of HSAF on the survival of experimental mice infected with *C. albicans* was carried out. A significant increase in the mice treated with HSAF (26 days) compared to vehicle mice (14 days) and mice treated with AMB (22 days) and FLU (24 days) was observed. Microscopic examination of kidney sections showed numbers of pyogranulomatous inflammatory foci in the vehicles, while HSAF treatment reduced the lesions of organ tissue. The results showed that HSAF significantly decreased the fungal burdens in the kidneys of mice and also tended to prolong the survival of the infected animals.

Discussion

C. albicans is a common opportunistic fungal pathogen of humans. Disseminated invasive candidiasis has an estimated mortality rate of 40%, even with the use of antifungal drugs due to its toxicity, high price and drug resistance.[35] Therefore, the development of effective antifungal agents and therapies is urgently needed. Recently, ROS has been focused on, due to their pivotal role in the apoptosis of many different cell types. Previous studies have shown that several stimuli, such as acetic acid,[36] resveratrol,[37] farsenol[38] and antimicrobial peptides[39] caused *C. albicans* cells to undergo apoptosis through ROS dependent pathway. ROS accumulation is considered to be a typical hallmark of apoptosis. These previous reports prompted us to determine whether HSAF induced the apoptosis through ROS dependent pathway.

In this study, the transcriptional sequencing and analysis treating with DMSO and HSAF using Ⅱlumina 2000 assembly technology and RNA-Seq quantification analysis were performed. Downstream events, measured by high-content imaging, and flow cytometry, showed a dramatic increase in mitochondrially produced ROS and subsequent DNA damage with up regulation of related proteins. Based on transcriptional sequencing and analysis, the important regulatory genes involved in the ROS and apoptosis pathway were identified. These results will be helpful for illuminating the mechanisms of HSAF on the fungi. To examine the role of HSAF induced ROS in fungal cell death, ROS production was blocked by adding antioxidants to HSAF-treated cultures. The addition of antioxidants increased the survival of cultures treated with HSAF, indicating that HSAF caused ROS-induced

fungal cell death. Antioxidant enhancements protect cells treated with HSAF against apoptosis, indicating that ROS are not a meaningless side effect of mitochondrial disintegration but a key regulator to yeast apoptosis. HSAF belonged to PTMs, which is distinct from any existing fungicides. To our knowledge, this is the first study of PTMs causing apoptosis through ROS dependent apoptotic pathway in *C. albicans*.

In conclusion, HSAF, a natural product, induced apoptosis in *C. albicans* through ROS dependent pathway. We also found that HSAF inhibited tubulin polymerization in vitro. The MD studies revealed that β-tubulin maybe the target of HSAF against *C. albicans*, but it need to be confirmed in future study. Nevertheless, HSAF could be considered as a potential lead in the development of a novel class of antifungal agents. It shed light on possible medical applications involving HSAF in particular for the treatment of *C. albicans* infections.

Acknowledgement

This work was supported by National Key Basic Research Program of China (973 Program) (2012CB721005, 2013CB734002), Joint Research Fund for Overseas Chinese, Hong Kong and Macao Young Scholars to Y. S. & L. D. (31329005), the State Key Program of National Natural Science Foundation of China (81530091), the NIH (R01AI097260), Natural Science Foundation of Shandong Province, China (ZR2013HQ048), Program for Changjiang Scholars and Innovative Research Team in University (IRT13028) and National Natural Science Funds for Distinguished Young Scholars to Y. S. (30325044).

Notes and references

1. P. Belenky, D. Camacho and J. J. Collins, *Cell Rep*, 2013, **3**, 350-358.
2. H. Hof, *Mycoses*, 2006, **49**, 2-6.
3. N. D. Grover, *Indian J. Pharmacol.*, 2010, **42**, 9.
4. J. H. Hwang, H. Choi, A. R. Kim, J. W. Yun, R. Yu, E. R. Woo and D. G. Lee, *J. Appl. Microbiol.*, 2014, **117**, 1400-1411.
5. J. C. S. Brown, J. Nelson, B. VanderSluis, R. Deshpande, A. Butts, S. Kagan, I. Polacheck, D. J. Krysan, C. L. Myers and H. D. Madhani, *Cell*, 2014, **159**, 1168-1187.
6. Y. Li, J. Huffman, Y. Li, L. Du and Y. Shen, *Med. Chem. Commun.*, 2012, **3**, 982-986.
7. L. Lou, H. Chen, R. L. Cerny, Y. Li, Y. Shen and L. Du, *Biochemistry*, 2011, **51**, 4-6.
8. S. G. Cao, J. A. V. Blodgett and J. Clardy, *Org. Lett.*, 2010, **12**, 4652-4654.
9. S. Li, L. Du, G. Yuen and S. D. Harris, *Molecular Biology of the Cell*, 2006, **17**, 1218-1227.
10. I. Keren, Y. Wu, J. Inocencio, L. R. Mulcahy and K. Lewis, *Science*, 2013, **339**, 1213-1216.
11. M. A. Kohanski, D. J. Dwyer, J. Wierzbowski, G. Cottarel and J. J. Collins, *Cell*, 2008, **135**, 679-690.
12. A. W. Fothergill, 2012, DOI: 10.1007/978-1-59745-134-5_2, 65-74.
13. T. G. Brayman and J. W. Wilks, *Antimicrob. Agents Chemother.*, 2003, **47**, 3305-3310.
14. B. Hwang, J.-S. Hwang, J. Lee and D. G. Lee, *Biochem. Biophys. Res. Commun.*, 2011, **405**, 267-271.
15. A. J. Phillips, I. Sudbery and M. Ramsdale, *Proceedings of the National Academy of Sciences*, 2003, **100**, 14327-14332.
16. C. Park and D. G. Lee, *Biochem. Biophys. Res. Commun.*, 2010, **394**, 170-172.
17. K. Arnold, L. Bordoli, J. Kopp and T. Schwede, *Bioinformatics*, 2006, **22**, 195-201.
18. N. Guex, M. C. Peitsch and T. Schwede, *Electrophoresis*, 2009, **30 Suppl 1**, S162-173.
19. F. Kiefer, K. Arnold, M. Kunzli, L. Bordoli and T. Schwede, *Nucleic Acids Res*, 2009, **37**, D387-392.
20. M. Biasini, S. Bienert, A. Waterhouse, K. Arnold, G. Studer, T. Schmidt, F. Kiefer, T. Gallo Cassarino, M. Bertoni, L. Bordoli and T. Schwede, *Nucleic Acids Res*, 2014, **42**, W252-258.
21. D. A. Case, T. E. Cheatham, 3rd, T. Darden, H. Gohlke, R. Luo, K. M. Merz, Jr., A. Onufriev, C. Simmerling, B. Wang and R. J. Woods, *J. Comput. Chem.*, 2005, **26**, 1668-1688.
22. A. W. Sousa da Silva and W. F. Vranken, *BMC Res. Notes*, 2012, **5**, 367.
23. P. Pozzatti, E. S. Loreto, D. A. N. Mario, L. Rossato, J. M. Santurio and S. H. Alves, *J. Mycol. Med.*, 2010, **20**, 185-189.
24. H. Liu, M. Sun, D. Du, H. Pan, T. Cheng, J. Wang and Q. Zhang, *PLoS ONE*, 2015, **10**, e0128009.
25. C. P. Baines, R. A. Kaiser, N. H. Purcell, N. S. Blair, H. Osinska, M. A. Hambleton, E. W. Brunskill, M. R. Sayen, R. A. Gottlieb and G. W. Dorn, *Nature*, 2005, **434**, 658-662.
26. N. Vanlangenakker, T. V. Berghe and P. Vandenabeele, *Cell Death & Differentiation*, 2011, **19**, 75-86.
27. S. G. Zebell and X. Dong, *Cell host & microbe*, 2015, **18**, 402-407.
28. C. Muñoz-Pinedo, in *Self and Nonself*, Springer, 2012, pp. 124-143.
29. A. Weingärtner, G. Kemmer, F. D. Müller, R. A. Zampieri, M. G. dos Santos, J. Schiller and T. G. Pomorski, *PLoS ONE*, 2012, **7**, e42070.
30. P. A. Leventis and S. Grinstein, *Annual review of biophysics*, 2010, **39**, 407-427.

31. B. Hao, S. Cheng, C. J. Clancy and M. H. Nguyen, *Antimicrob. Agents Chemother.*, 2013, **57**, 326-332.
32. J. H. Hwang, I.-s. Hwang, Q.-H. Liu, E.-R. Woo and D. G. Lee, *Biochimie*, 2012, **94**, 1784-1793.
33. F. Mollinedo and C. Gajate, *Apoptosis : an international journal on programmed cell death*, 2003, **8**, 413-450.
34. K. D. Shin, Y. J. Yoon, Y. R. Kang, K. H. Son, H. M. Kim, B. M. Kwon and D. C. Han, *Biochem. Pharmacol.*, 2008, **75**, 383-394.
35. Y. Lu, C. Su and H. P. Liu, *Trends Microbiol.*, 2014, **22**, 707-714.
36. A. J. Phillips, I. Sudbery and M. Ramsdale, *Proc. Natl. Acad. Sci. U. S. A.*, 2003, **100**, 14327-14332.
37. J. Lee and D. G. Lee, *Curr. Microbiol.*, 2014, DOI: 10.1007/s00284-014-0734-1.
38. J. Zhu, B. P. Krom, D. Sanglard, C. Intapa, C. C. Dawson, B. M. Peters, M. E. Shirtliff and M. A. Jabra-Rizk, *PLoS One*, 2011, **6**, e28830.
39. J. Cho and D. G. Lee, *Biochim. Biophys. Acta*, 2011, **1810**, 1246-1251.

Figure legends

Fig. 1. Structure of HSAF (A); Antifungal activities of HSAF. HSAF effected on mycelial growth of fungus at the dose of 0, 5, 10, 15 and 20 μg/mL in vitro. Photographs indicating petri dishes containing each fungal species including *P. grisea*, *F. verticillioide, R. solani* and *S. sclerotiorum* were taken by digital camera at 5 days after inoculation of conidia (B); HSAF inhibited the tube of *C. albicans*. Stained by crystal violet and observed under a fluorescent microscope. The cultures were incubated for 48 h in RPMI 1640 medium at 25 °C without shaking, the cells were treated with DMSO, 1.5, 3 and 6 μg/mL HSAF at 37 °C for 4 h, HSAF inhibited the yeast-to-hyphal transformation at low concentration with 6 μg/mL, Scale bar, 10 μm (C).

Fig. 2. Gene expression differences among the different samples. The correlation scatter plot of gene expression was difference in response to HSAF at 10 μg/mL for 10 h (A); Histogram presentation of Gene Ontology classifications. The results were summarized in three main categories: biological processes, cellular components, and molecular functions with 10 μg/mL HSAF treating for 10 h. The x-axis on the right side shows the number of genes (B); A heat-map showed transcription factor family genes that were differentially expressed protein levels of energy metabolism, cell growth and death pathway in response to HSAF at 10 μg/mL for 10 h. The color scale indicates fold-change in gene expression. Yellow indicates high expression and blue indicates low expression (C).

Fig. 3. HSAF-Dependent ROS production led to fungal cell death. Histograms showed the fluorescence intensity of incubated with DCFH-DA. Cells treated with 3, 6 and 12 μg/mL HSAF for 1, 2 and 3 h (A). Changes in mitochondrial membrane potential. Cells were treated with DMSO, 3, 6 and 12 μg/mL HSAF for 3 h. Stained with $DiOC_6(3)$ and analyzed by flow cytometry (B). ROS scavenging agents reduces the antifungal activity of HSAF against *C. albicans*. Scavengers diminished the toxicity of HSAF by 4-fold for 0.5 mM AA and by 2-fold for 0.5 mM NAC and GSH. Log of CFU/ml remaining after drug exposure in the presence and absence of 0.5 mM Vc or TU at 12 μg/mL HSAF.

Fig. 4. HSAF induces the early and late apoptosis in *C. albicans*. Cells treated with 3, 6, 12 and 24 μg/mL HSAF at 4, 8 h shown by FITC-Annexin-V / PI staining (A) and by TUNEL staining (B). Cells treated with DMSO, 10 μg/mL AMB, 24 μg/mL HSAF , 24 μg/mL HSAF + 1 mM Vc, 24 μg/mL HSAF + 5 mM Vc shown by FITC-Annexin-V / PI (C), DAPI staining (D) and TUNEL staining (E) and observed under a fluorescent microscope. Bar, 10 μm.

Fig. 5. Influence of HSAF on purified tubulin polymerization in vitro. The tubulins were incubated at 37 °C in the presence of DMSO, 10 μM HSAF and 10μM vincristine and microtubule formation was measured by the spectrophotometer. Absorbance at 340 mm was monitored (A). Plot of RMSD (in ångstrom) for the β-tubulin-HSAF complex during 20 ns MD simulation (B). The detailed interactions between HSAF and β-tubulin of *C. albicans* wild type and HSAF selectively occupies the eleven key residues binding site of the β-tubulin wild type (C).

Fig. 6. Macroscopic inflammation of kidney taken from mice infected with *C. albicans* SC5314, the mice were infected by injection of a 100 μL inoculum containing 1×10^6 cells of *C. albicans* SC5314 via the lateral tail vein (A). The kidney burden analysis of infected mice receiving indicated treatments (B). Survival curve of BALB/c mice infected by *C. albicans* SC5314 (C). Pathology of kidney taken from mice infected with *C. albicans* SC5314. The kidneys of mice were excised from the infected model group with no treatment (1), and the groups treated with DMSO (2), AMB (3), FLU (4) and HSAF (5) on the 3th days of infection. The images of hematoxylin-eosin (D) or periodic-acid schiff (E) stained sections are presented at 200×magnification, Bar = 3 μm.

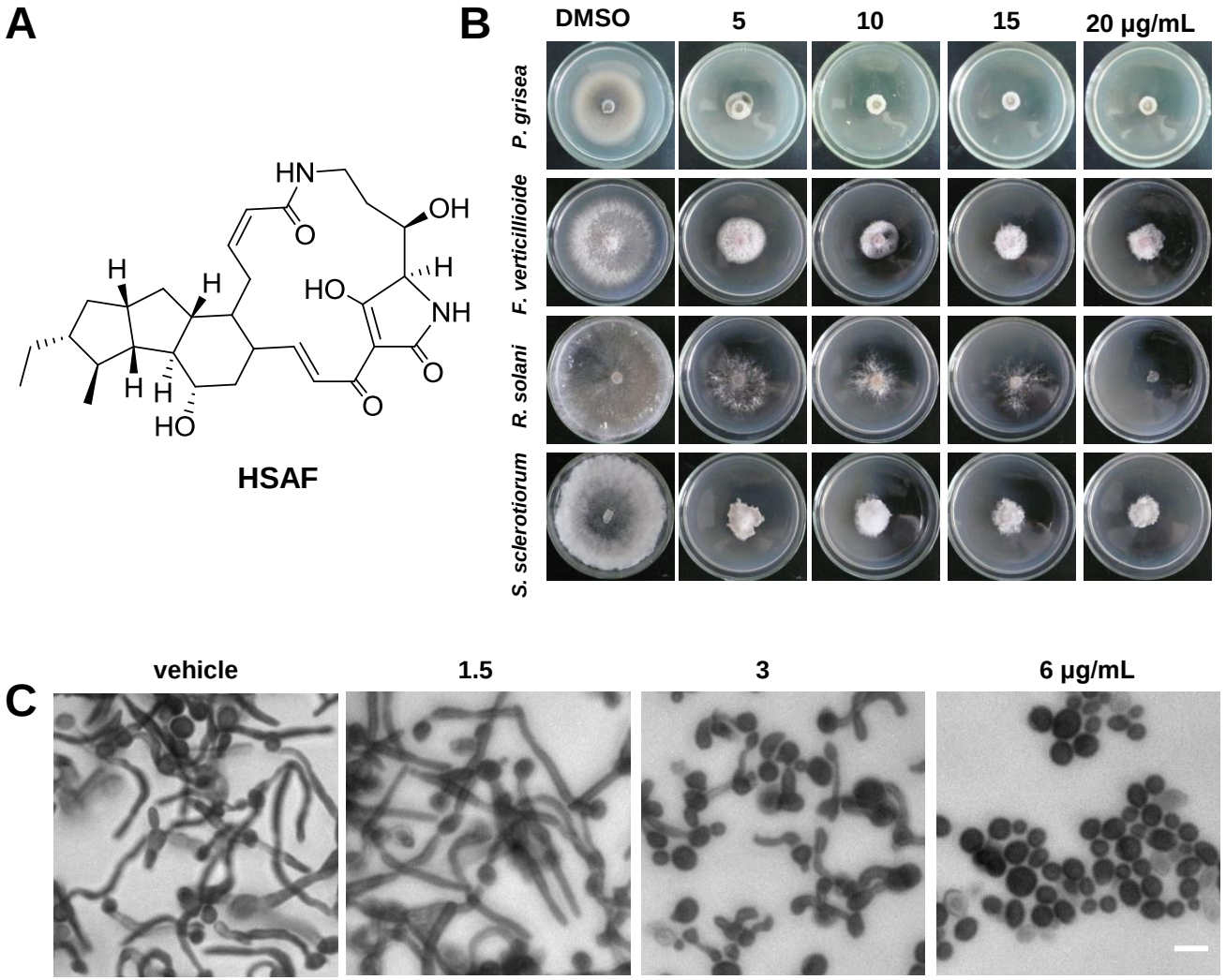

Figure 1

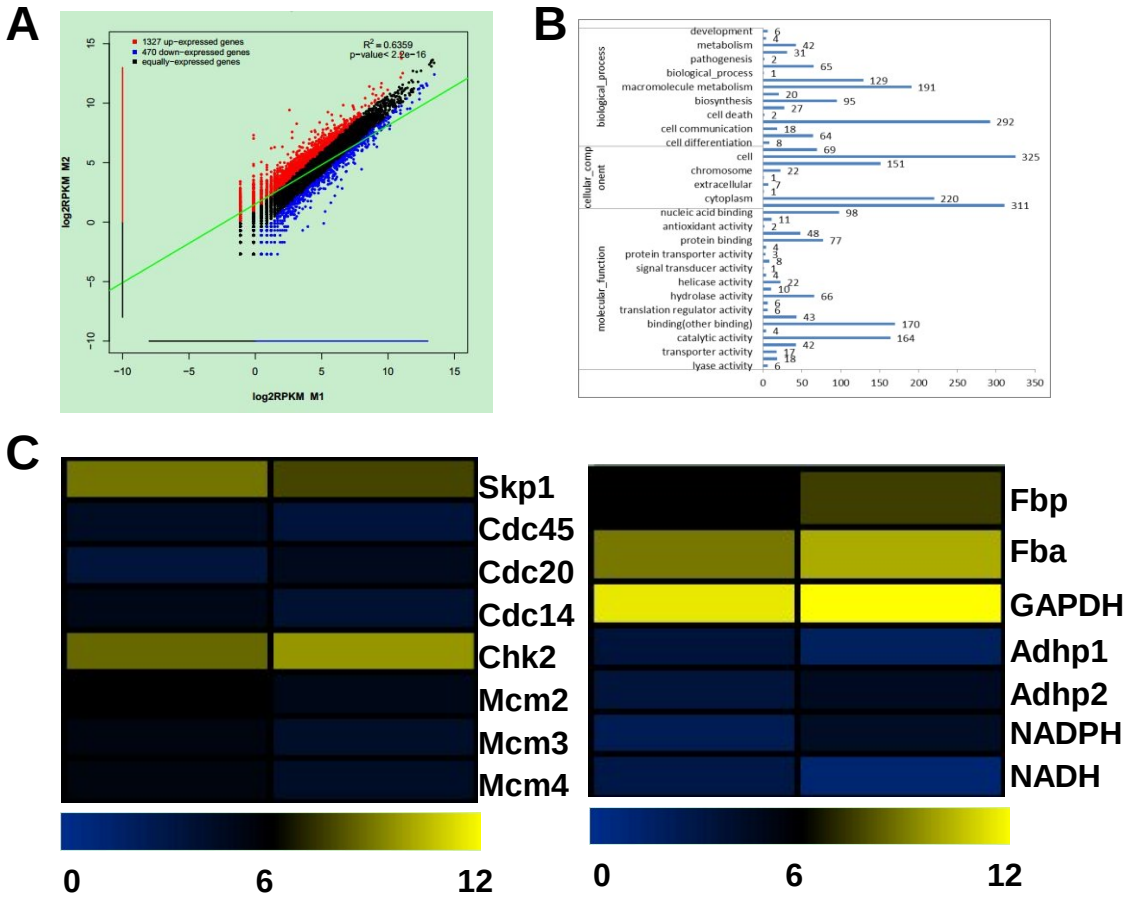

Figure 2

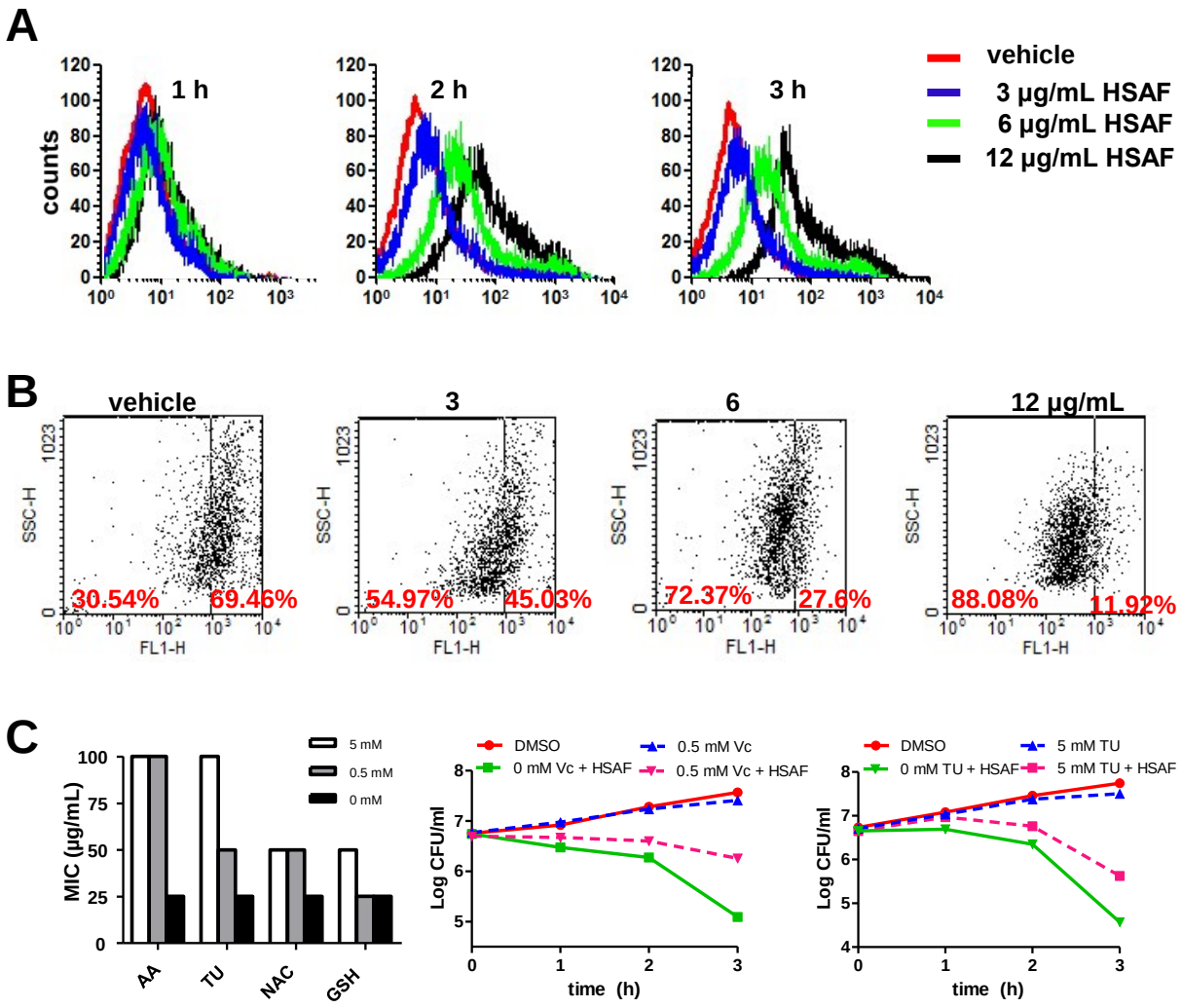

Figure 3

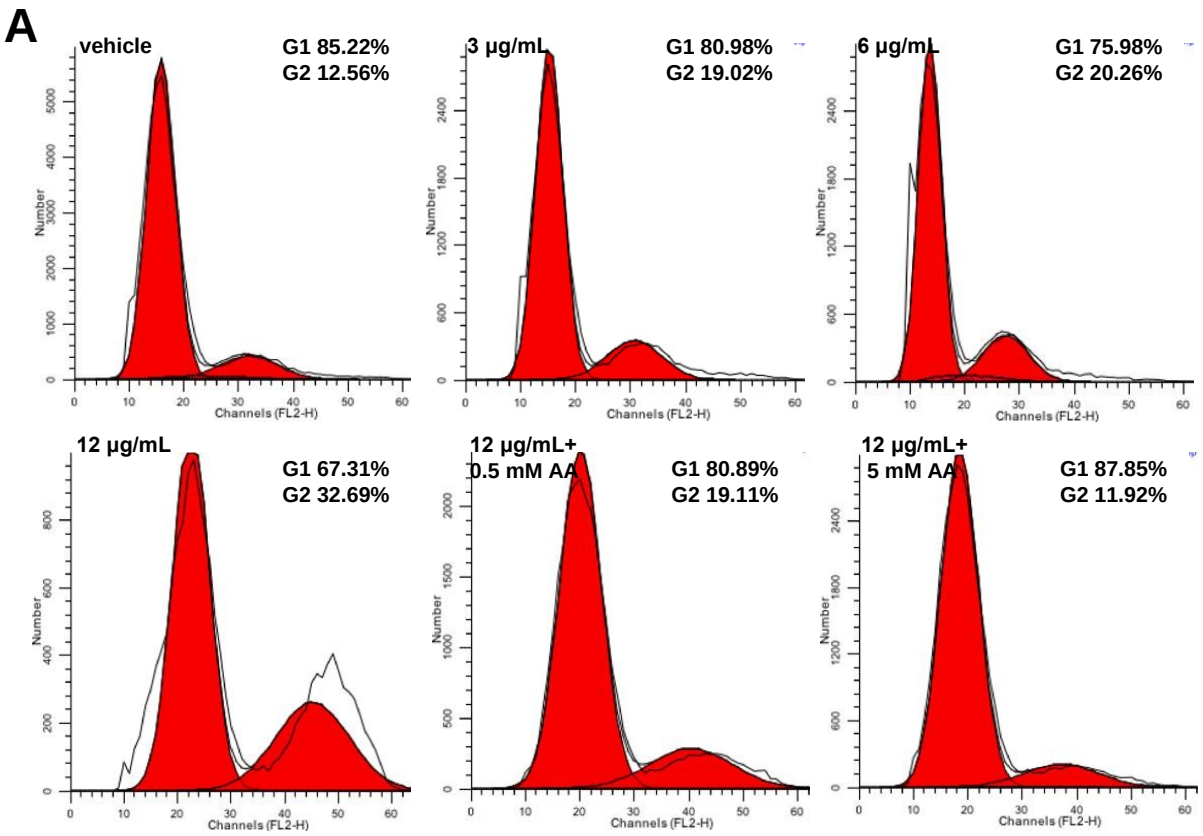

Figure 4

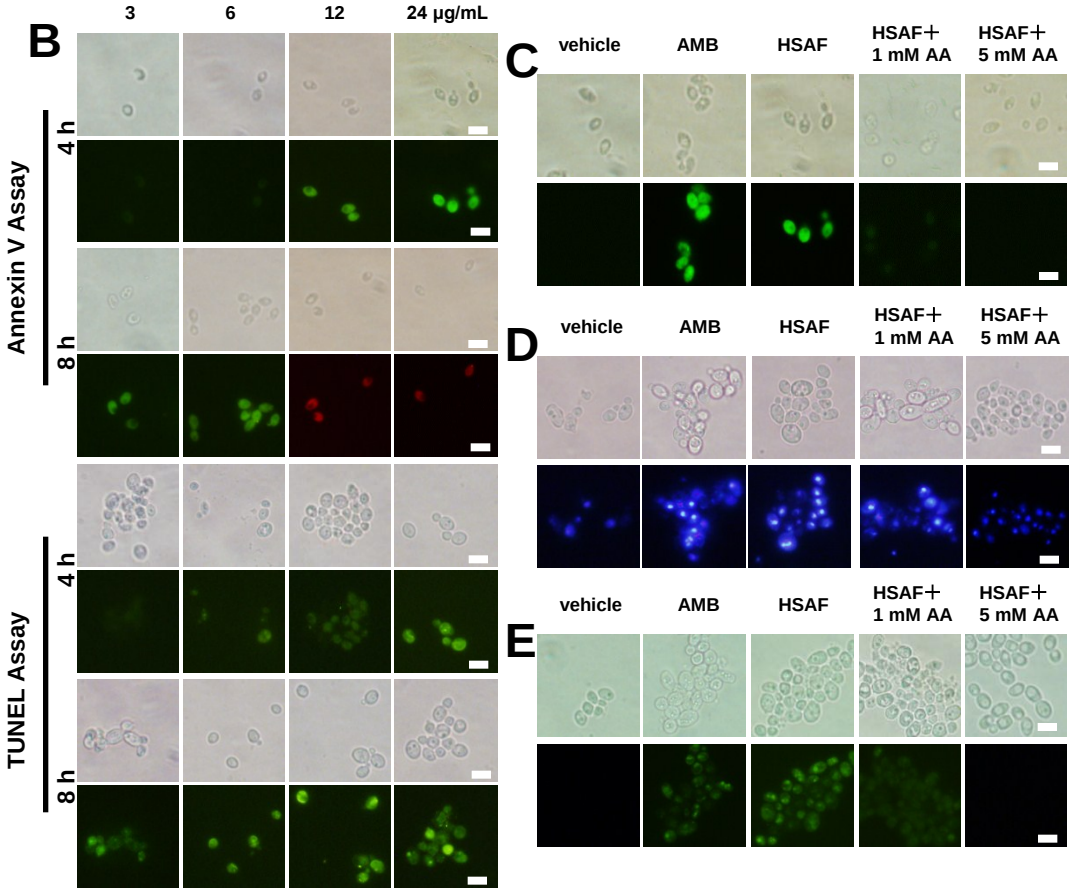

Figure 4

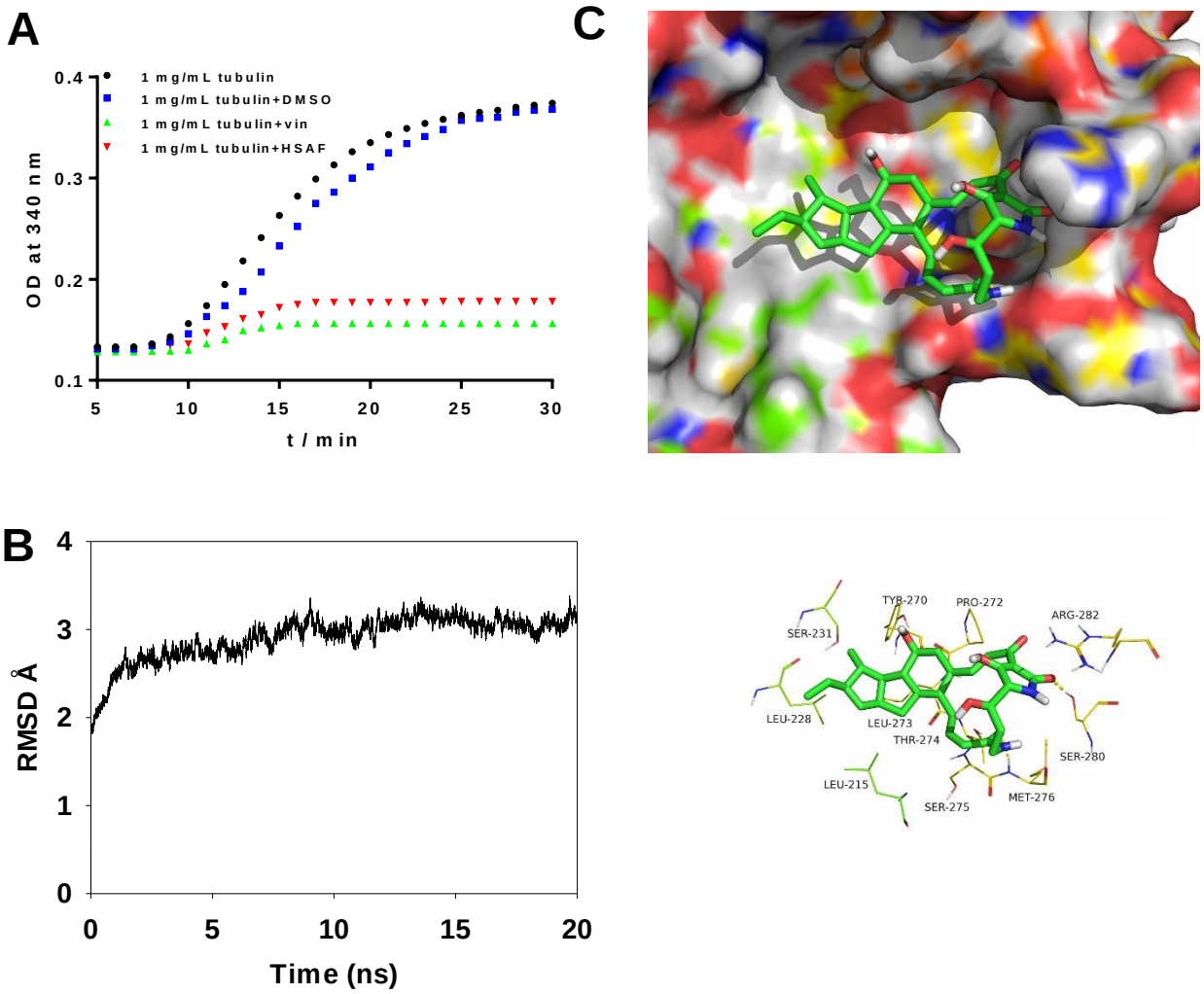

Figure 5

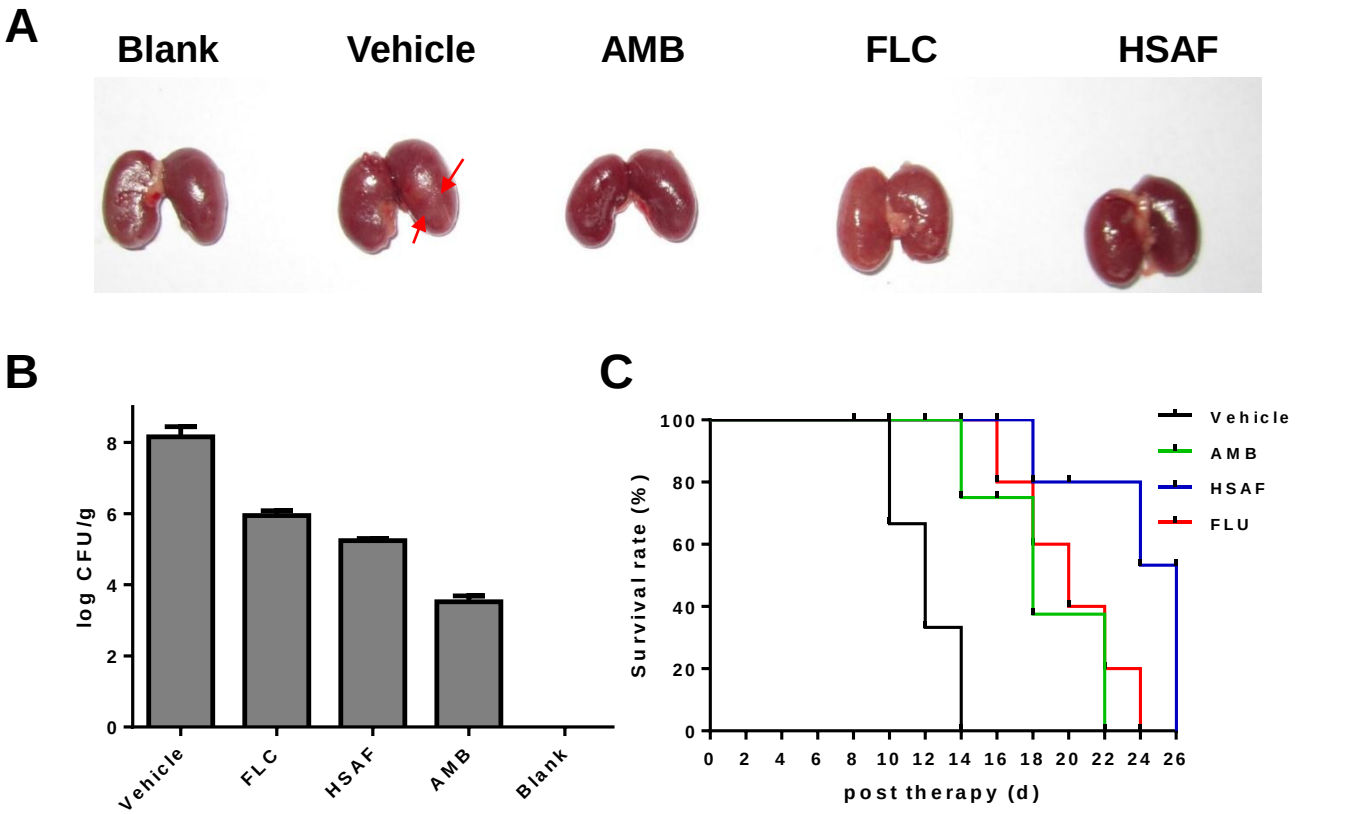

Figure 6

Graphical Abstract

HSAF, isolated from *Lyaobacter enzymogenes* C3, was a potent antifungal with a broad spectrum of activity. HSAF induced the apoptosis of *Candida albicans* through inducing the production of reactive oxygen species (ROS). The binding model of HSAF to β-tubulin was simulated by Amber12 and shown by PyMoL.